METHODS AND APPLICATIONS

Engineering deamidation-susceptible asparagines leads to improved stability to thermal cycling in a lipase

K. Bhanuramanand, Shoeb Ahmad, and N. M. Rao*

Centre for Cellular and Molecular Biology (CSIR-CCMB), Hyderabad 500007, India

Received 29 May 2014; Revised 9 July 2014; Accepted 10 July 2014
DOI: 10.1002/pro.2516
Published online 14 July 2014 proteinscience.org

Abstract: At high temperatures, protein stability is influenced by chemical alterations; most important among them is deamidation of asparagines. Deamidation kinetics of asparagines depends on the local sequence, solvent, pH, temperature, and the tertiary structure. Suitable replacement of deamidated asparagines could be a viable strategy to improve deamidation-mediated loss in protein properties, specifically protein thermostability. In this study, we have used nano RP-HPLC coupled ESI MS/MS approach to identify residues susceptible to deamidation in a lipase (6B) on heat treatment. Out of 15 asparagines and six glutamines in 6B, only five asparagines were susceptible to deamidation at temperatures higher than 75°C. These five positions were subjected to site saturation mutagenesis followed by activity screen to identify the most suitable substitutions. Only three of the five asparagines were found to be tolerant to substitutions. Best substitutions at these positions were combined into a mutant. The resultant lipase (mutC) has near identical secondary structure and improved thermal tolerance as compared to its parent. The triple mutant has shown almost two-fold higher residual activity compared to 6B after four cycles at 90°C. MutC has retained more than 50% activity even after incubation at 100°C. Engineering asparagines susceptible to deamidation would be a potential strategy to improve proteins to withstand very high temperatures.

Keywords: lipase; deamidation; mass spectrometry; site saturation mutagenesis; thermal cycling; asparagines

Abbreviations: bis-ANS, 1,1′,-bis(4-anilino)naphthalene-5,5′-disulphonic acid; CD, circular dichroism; CID, collision induced dissociation; dNTP, deoxyribonucleotide triphosphate; DTT, dithiothretol; ESI, electrospray ionization; IEF, isoelectric focusing; IPG, immobilized pH gradient; IPTG, isopropyl-β-d-thiogalactopyranoside; Kcat, turnover number; Km, Michaelis constant; LB, Luria Bertani; MS/MS, tandem mass spectrometry; PAGE, polyacrylamide gel electrophoresis; PCR, polymerase chain reaction; RA, residual activity; SDS, sodium dodecyl sulphate; SSM, site saturation mutagenesis.

Additional Supporting Information may be found in the online version of this article.

Grant sponsor: UGC (fellowship to K.B.R.). Grant sponsor: CSIR; Grant number: BSC0120.

Shoeb Ahmad's current address is: Laboratoire d'Enzymologie at Biochimie Structurales (LEBS), Centre de Recherche de Gif, CNRS, Bat 34, 1, avenue de la Terrasse, 91198 Gif sur Yvette, France.

*Correspondence to: N. Madhusudhana Rao, Centre for Cellular and Molecular Biology (CSIR-CCMB), Uppal Road, Hyderabad 500039, India. E-mail: Madhu@ccmb.res.in

Introduction

Proteins that withstand high temperatures have exciting biotechnological applications. Understanding of physical basis of thermostability in proteins has charmed protein chemists for a long time. The free energy of destabilization in proteins is very small (5–10 kcal) and is determined by a few weak interactions in the back ground of large number of interactions.[1] Several studies cataloged the differences between natural and *in vitro* evolved proteins that are stable at extremes of temperatures and demonstrated that simple hydrogen/ionic interactions and hydrophobic packing were sufficient to enhance thermostability.[1,2] These studies further concluded that the position and nature of these stabilizing interactions could be structure specific and are very challenging to predict using bioinformatics approaches. These comparative studies have provided several important generalities on abundance, or lack thereof, of various amino acids in extremes of temperature. Few studies have identified that amino acids such as serine, threonine, glutamine, and lysine[3] are less preferred in thermophiles, whereas glutamate and leucine[4] are less preferred in psychrophiles.

Exposure to high temperatures destabilizes the weak interactions in proteins leading to denaturation, which could be reversible in the absence of aggregation. In addition, high temperatures could also cause chemical changes in the protein. Deamidation of asparagines and glutamines is the most prominent nonenzymatic chemical reaction that is significantly enhanced at higher temperatures and physiological pH.[5,6] Deamidation results in an addition of negative charge to the residue resulting in alterations in protein interactions, which could affect the activity or refolding.[7,8] Interest in deamidation has gained importance since the extent of deamidation was associated with aging,[9,10] cataract formation,[9,11,12] immune recognition,[13] shelf-life of protein pharmaceuticals such as antibodies,[9,13,14] and so on.

Deamidation of asparagines is initiated by the cyclization reaction, which occurs between the carboxyl group of the asparagine and amide nitrogen of carboxyl side amino acid ($n+1$) followed by deamination resulting in the formation of succinimide intermediate. Hydrolysis of the intermediate could occur either at α-carboxamide or β-carboxamide resulting in the formation of aspartyl or iso-aspartyl products.[15,16] The relative proportions of aspartyl to iso-aspartyl products is under kinetic and thermodynamic control.[17] Based on a large number of model pentapeptide deamidation kinetics, it is well understood that the rate of deamidation of asparagine is significantly determined by the neighbouring amino acids especially the carboxyl side ($n+1$) amino acid.[18–21] The three-dimensional structure, pH, buffer salts, and solvent properties also could influence the rate of deamidation.[18,22] Hence different asparagines or glutamines in a protein may show high variability in their deamidation kinetics. Thus temperature-induced loss of function in proteins could depend on the extent of deamidation in a protein. Therefore, it is possible that by selectively replacing only those asparagines that are susceptible to deamidation, the thermotolerance of a protein could be improved.

Although substantial information is available on deamidation-mediated loss in protein properties, that is, aggregation, stability, activity, most of the mutational studies were limited to site-directed mutagenesis with aspartate[7,23,24] and glutamate[7,25] and rarely glycine, alanine, and serine.[8,26] These studies have focused on explaining functional consequences of deamidation. However, strategies which can simultaneously address impact of deamidation on protein function and provide most optimal solution to improve the property are necessary. Site saturation mutagenesis (SSM) approach has been used successfully in the recent past to understand the structure–function relationship and also to improve stability of proteins under a variety of *in vitro* evolution context.[27–30] Thus, a thorough analysis by SSM would seek optimal substitution for residue susceptible to deamidation to improve the thermotolerance of the protein.

We have earlier reported a variant of lipase from *Bacillus subtilis* that was evolved by directed evolution methods with exceptional thermostable properties.[31] This lipase variant, named as 6B, loses activity on exposure to high temperatures (>75°C), although there is no loss of protein due to aggregation. Shifts in pI to lower pH values upon heat treatment of 6B suggested the presence of residues susceptible to deamidation. In this study, we have identified the deamidated asparagines in heat-treated lipase 6B by mass spectrometry and selectively replaced the labile positions with a suitable amino acid by performing a site saturation mutagenesis on identified deamidation positions. By combining the best substitutions at three positions, a mutant lipase was designed that recovered its activity even after several heat/cool cycles compared to its parent (6B).

Results

Temperature-induced deamidation and loss of activity in lipase (6B)

Lipase 6B is an evolved lipase from *LipA* gene product in *Bacillus subtilis*. Methods of directed evolution were used to identify the mutations incorporated in 6B. Properties of lipase 6B were extensively investigated and reported earlier.[31,32] The midpoint of melting transition for 6B is 78.2°C. Upon

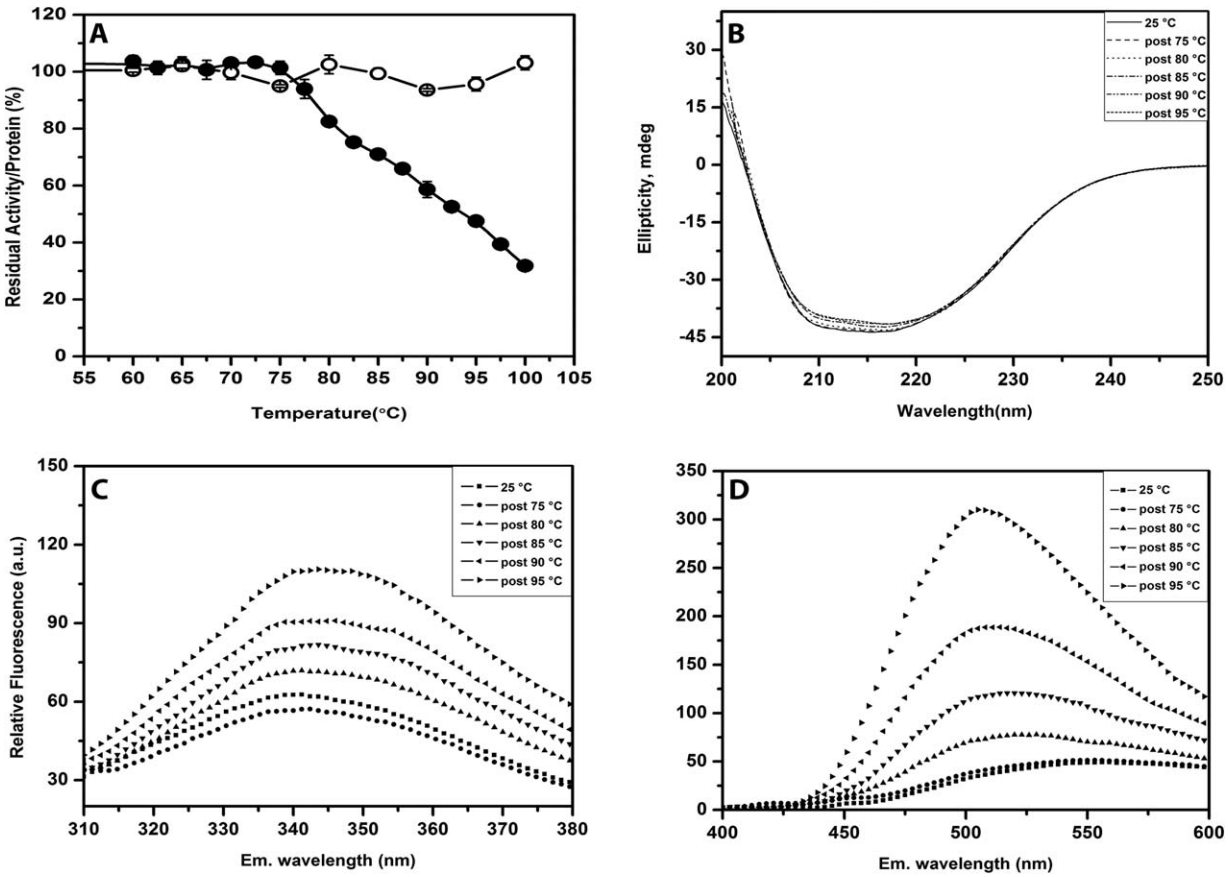

Figure 1. Characterization of 6B upon incubation at elevated temperature. (A): Residual activity (●) and soluble protein concentration (o) of 6B at various temperatures. 6B protein, heated to various temperatures (75–95°C) and cooled to room temperature, was monitored by Far-UV CD (B), intrinsic tryptophan fluorescence (C), and bis-ANS binding (D). Samples incubated at 25°C were treated as control.

incubation of 6B at temperatures 75°C and above, a steady decrease in activity of lipase was observed. This loss of activity was not due to the denaturation-mediated aggregation, since most of the protein was found in the supernatant upon centrifugation [Fig. 1(A)]. 6B upon heat denaturation and cooling does not show any alterations in its secondary structure compared to untreated 6B [Fig. 1(B)]. Intrinsic tryptophan fluorescence, an indicator of tertiary structure in proteins, of 6B has significantly increased on heat treatment. One of the two tryptophans is buried in lipase while another one is surface exposed. Fluorescence emission remains quenched for tryptophans in native state. Fluorescence dequenching associated with a red shift in heat-treated and refolded samples suggest that the environment of tryptophans has altered and became more polar [Fig. 1(C)]. This observation was further corroborated by enhanced binding of 4,4′-dianilino-1,1′-binaphthyl-5,5′-disulfonic acid (bis-ANS) to the protein after heat treatment [Fig. 1(D)]. A 10-fold increase in fluorescence followed by a blue shift in emission maximum of bis-ANS indicates that the protein has more surface hydrophobicity than the untreated protein. These studies suggest while the protein remained soluble and retained secondary structure, the protein has not regained the native tertiary structure as indicated by loss of activity, increase in tryptophan fluorescence and enhanced bis-ANS binding.

Inability of the protein to achieve native structure on incubation at elevated temperature inspite of its nonaggregating nature could be attributed to temperature-induced chemical modifications. To

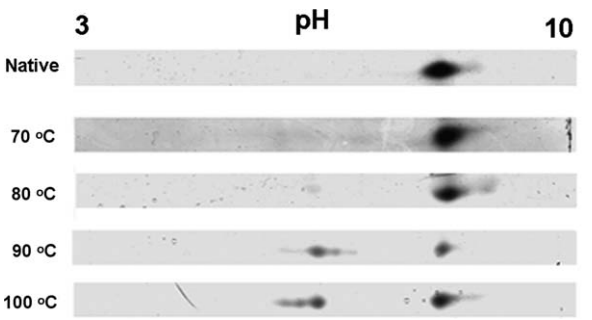

Figure 2. IEF of 6B. Heated and unheated (top) 6B protein was isoelectrofocused on an IPG strip with pI gradient from 3 to 10. IPG strip was run in second dimension on SDS-PAGE gel and was stained with Coomassie.

probe deamidation status in 6B lipase, shifts in pI were monitored. The heat-treated samples of 6B (70–100°C) were subjected to isoelectric focusing (IEF). Untreated 6B has a pI of 8.2, and the pI of the refolded (heat treated) 6B has shifted to lower pH values. The intensity of low pH spot has increased with increase in incubation temperature, with a corresponding decrease in the intensity of pH 8.2 spot (Fig. 2). Shift in the pI to low pH value indicates accumulation of additional negative charges in protein. In our previous studies, we have extensively tested and found that 6B does not undergo any detectable proteolysis upon heating. Exposure to high temperatures could have caused deamidation leading to shifts in pI and also prevented ability to regain native tertiary structure in 6B on refolding.

Identification of residues susceptible to deamidation on heat treatment by mass spectrometry

Deamidation rate in a protein is influenced by a many factors such as the primary sequence, tertiary structure, and also various parameters including ionic strength, pH, solvent exposure, temperature, and so on. It has been observed that deamidation of glutamine is slower compared to asparagine.[9] Based on model pentapeptide studies, the deamidation kinetics of asparagines can vary by several thousand folds.[21] It is essential to identify susceptible residues to explain the inability of the lipase to refold to native state upon heat treatment and subsequent cooling. Deamidation of asparagines in a protein results in a mass shift of 0.984 Da. Thus, deamidated peptide could be easily identified with high accuracy by mass spectrometry. However, long incubation times during proteolysis[33] and a reduction step with iodoacetamide performed at 55–60°C for 1 h may also result in deamidation. Modified work flows are being developed to avoid process-induced deamidation.[34–36] In the case of 6B, incubation at 37°C during proteolysis did not result in deamidation, and reduction step is not required as 6B lipase does not have a cysteine. Most of the proteomic methods use electrospray ionization in combination with electron capture dissociation[37] or electron transfer dissociation[38] for qualitative determination of the product type, that is, aspartate or isoaspartate. Since our focus was on identifying positions susceptible to deamidation, we have used nano reverse phase-high performance liquid chromatography (RP-HPLC) electron spray ionization mass spectrometry (ESI MS/MS) with collision induced dissociation (CID) fragmentation mode.

6B was exposed to high temperatures (80°C, 90°C, and 100°C), and its deamidation pattern was analyzed by mass spectrometry as described in Materials and Methods section. From samples incubated at 80°C, majority of the peptide spectral matches

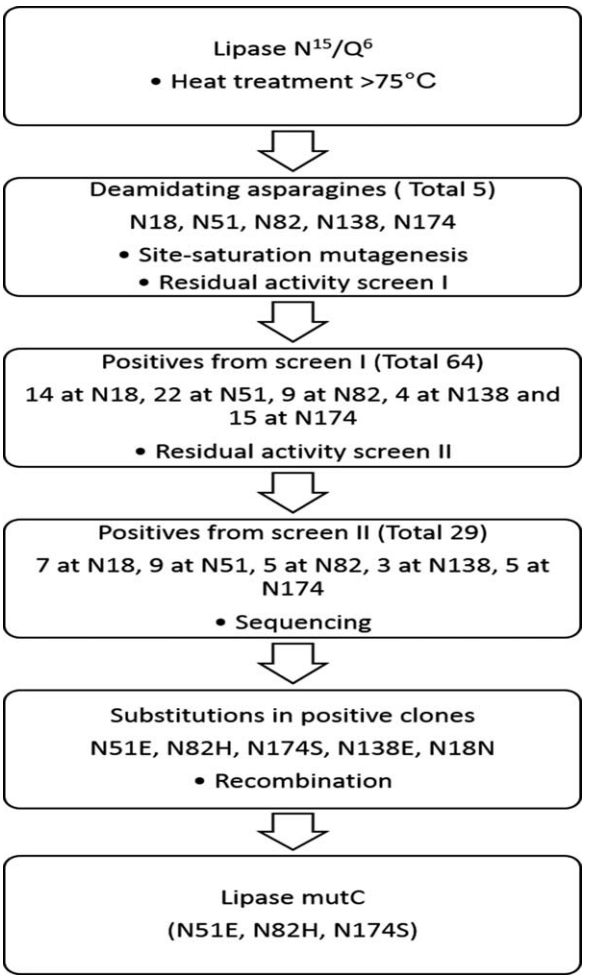

Figure 3. Work flow involving mass spectrometry and SSM to identify suitable replacements to deamidated asparagines.

corresponding to the peptide "45-TGTNYN**N**GPVLSR-57" (M+H 1393.67) showed deamidation at position 51 (bold), whereas deamidation of asparagines at positions N82, N18, N138, and N174 were seen only at 90°C and 100°C. Peptide fragment analysis indicated that susceptibility of asparagines to deamidation was temperature dependent and position specific (Supporting Information Table 1). Thus five asparagines corresponding to 18, 51, 82, 138, and 174 positions deamidated and thus may have led to the loss of activity in 6B upon heating.

SSM of five deamidated asparagines

We explored the possibility of replacing the deamidation-susceptible asparagines to improve the thermostability of lipase. In the published reports, the susceptible asparagines were mostly replaced with aspartic acid.[23–25,39] To identify the suitable amino acid replacement at these five positions, a SSM at these five positions was performed. The mutant library generated by SSM was screened by exposing the culture supernatants to 25°C, 85°C, and 95°C. Based on the ratio of residual activity at

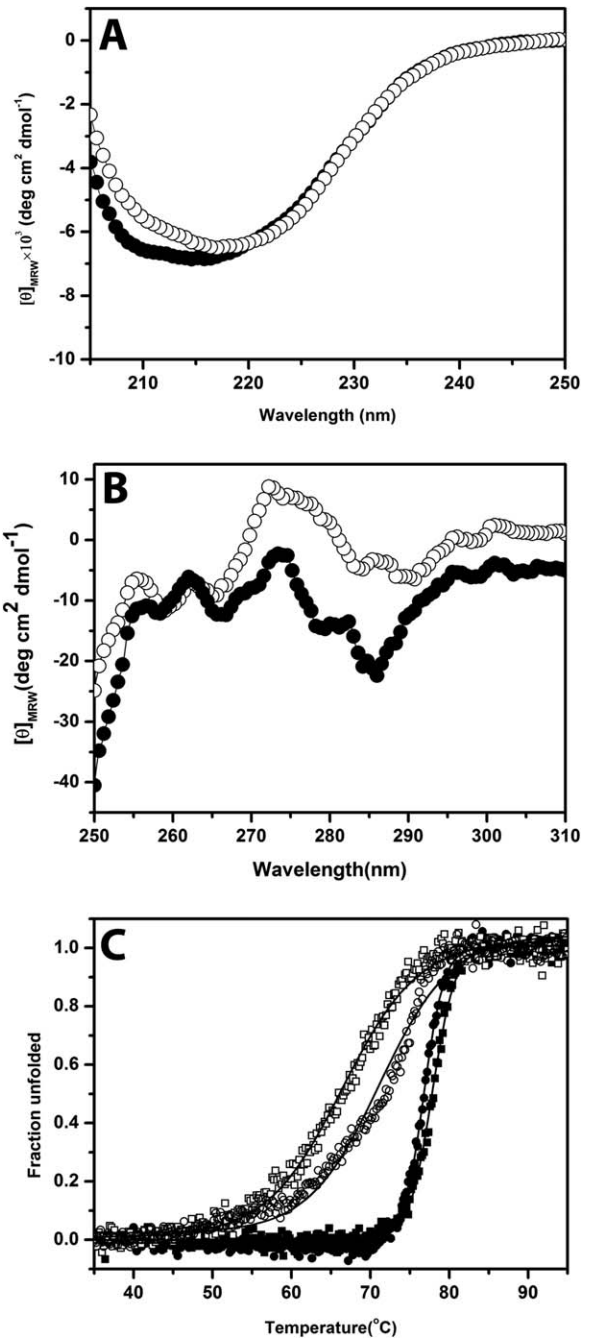

Figure 4. Characterization of 6B and mutC: (A) Far-UV CD spectra of 6B (●) and mutC (○) at 25°C. (B) Near-UV CD spectra of 6B (●) and mutC (○) at 25°C. (C) Unfolding (■, ●) and refolding (□, ○) of mutC (circle) and 6B (square) was monitored by change in ellipticity at 222 nm as a function of temperature.

high temperature to room temperature for 1000 clones (~200 for each position), 64 clones were selected after initial screening (14 mutants for N18, 22 mutants for N51, 4 mutants for N138, 9 mutants for N82, and 15 mutants for N174) (Fig. 3). Sixty-four transformants identified from the first screen were subjected to a second tier screen as described in Materials and Methods section. Twenty-nine clones for five positions (seven for N18, nine for N51, three for N138, five for N82, and five for N174) were identified. These mutants were sequenced to identify the amino acid substitutions. All substitutions at position 51 were with glutamates. Histidine and serine replacements at positions 82 and 174 have positively contributed to the activity. All positive substitutions at position 18 were asparagines. Aspartate was the most frequent substitution at position 138 and has shown a marginal improvement in residual activity. Based on the frequency of substitutions and residual activity measurements, we have chosen glutamate, histidine, and serine for substituting asparagines at 51, 82, and 174, respectively. We combined these three mutations in the background of 6B to generate mutC (6B with N51E+N82H+N174S). SSM approach and the observed optimal substitutions observed here suggest that substitution of asparagines susceptible to deamidation with aspartic acid may not be a best option.

Structure and activity of recombinant mutC

Secondary structure analysis of mutC by Far-UV suggested differences in the 208–210 nm region of the spectrum which indicate slightly altered packing of helix compared to 6B (Fig. 4A). This can be attributed to the fact that two of the three mutations 51 and 82 are in helix.

Near-UV CD spectra also shows slight shift in the peak corresponding to 280–290 nm indicating changes in the tyrosine environment (Fig. 4B). This is also true as peptides corresponding to these positions harbor tyrosine in their sequence (45-TGTN**Y**NNGP VLSR-57, 70-KVIDVAHSMGGANTL**YY**IK-88).

Temperature-induced unfolding and refolding of mutC and 6B was monitored by protein CD signal. Based on melting curve the $T_{m\ app}$ of mutC was found to be 1°C lower than 6B. However, fraction of secondary structure recovered on thermal cycling seems to be more for mutC compared to 6B (Fig. 4C). Absence of susceptible asparagines in mutC and replacement with suitable residues may have led to a decrease in unfavorable interactions which may have helped mutC to regain its structure upon thermal cycling.

Table I. *Enzyme Kinetics of 6B and mutC*

	Lipase	
Parameter	6B	mutC
Specific activity (μmoles pNP min−1 mg−1 of enzyme)	39.6	17.6
Km (mM)	0.49	0.59
Vmax (mM min−1)	0.31	0.14
Catalytic efficiency (mM−1 min−1)	1257	463

Kinetic parameters of 6B and mutC were estimated by assays using PNPA as substrate at 25°C.

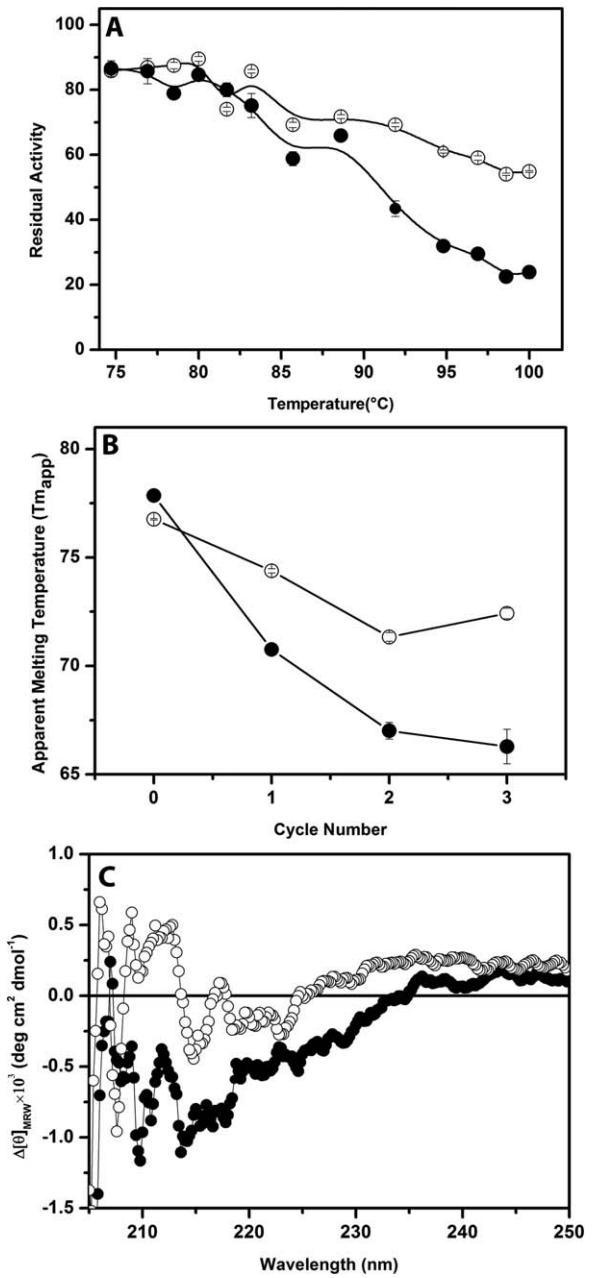

Figure 5. Thermal properties of 6B and mutC. (A) Residual activity of 6B (●) and mutC (○) were plotted after incubating at various temperatures and measuring activity at RT. (B) Apparent melting temperature ($T_{m\ app}$) of 6B (●) and mutC (○) after each heat/cool cycle. (C) Δ Ellipticity, that is, difference in ellipticity before and after three heat/cool cycles, of 6B (●) and mutC (○).

The catalytic parameters of 6B and mutC were estimated using *p*-nitrophenyl acetate (PNPA) as substrate. K_m shows a marginal increase in mutC (0.59) compared to 6B (0.49); however, the V_{max} value decreased by more than twofold resulting in an overall catalytic efficiency decrease by threefold in mutC compared to 6B (Table I). This may be attributed to the fact that H82 in mutC may have altered the interactions with positions 78 (next to active site serine77), 79, 80, 85, and 86 by main chain–main chain interactions. Position 78 is a methionine, a key member of oxyanion hole required for catalysis. Any perturbation in the α-chain at this position could lead to decrease in hydrolysis efficiency.

Thermotolerant properties of mutC

Thermal inactivation for mutC and 6B was monitored at temperatures ranging from 70 to 100°C, and the residual activity was plotted against temperature. MutC retained about 55% residual activity after incubation at 100°C whereas 6B showed only 23% of initial activity [Fig. 5(A)]. To evaluate the observed recovery, secondary structure in mutC translates to its improved ability to regain native tertiary structure, both mutC and 6B were subjected to three heat and cool cycles (Each cycle—85°C/30 min, 4°C/20 min, RT/20 min). Refolded proteins were analyzed for changes in the secondary structure and $T_{m\ app}$. As shown in Figure 5(C), the decrease in $T_{m\ app}$ was progressive in 6B, whereas it remained at 72°C for mutC after second cycle. After three cycles, $T_{m\ app}$ decrease in 6B was 11°C, whereas mutC experienced a reduction of 4.5°C. The secondary structure of 6B and mutC was obtained on samples before and after heat cycles. The Δ ellipticity profile shows that the differences in CD signals before and after heat cyles was signficanctly less in mutC compared to 6B [Fig. 5(D)].

Binding of bis-ANS to 6B and mutC before and after each cycle indicated an increase in binding of the fluorophore after each cycle with a marginally lesser binding with mutC after the second cycle (Supporting Information Fig. 1). Comparison of refolding behavior, higher $T_{m\ app}$ values after refolding, lesser bis-ANS binding along with smaller differences in the ellipticity in mutC compared to 6B indicate that mutC has ability to withstand higher temperatures.

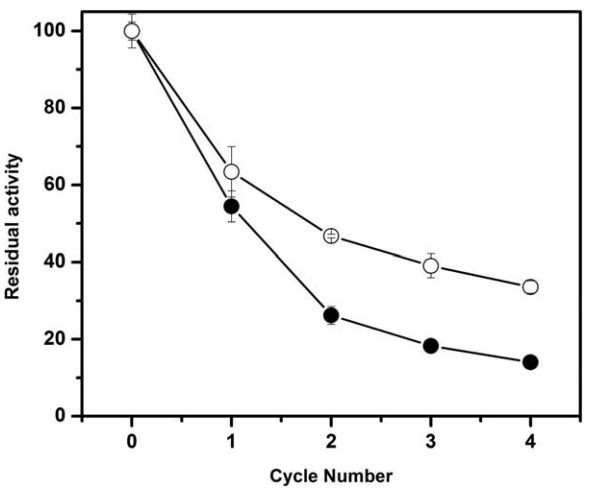

Figure 6. Residual activity of 6B (●) and mutC (○) as a function of heat cool cycles.

Residual activity and deamidation status in heat cycled mutC

To study the effect of improved thermal tolerance on activity, the activities of mutC and 6B were investigated after each refolding cycle to understand the protective role of mutations in mutC. Both the lipases were subjected to thermal exposure and cycling as described earlier, and the specific activity was plotted after each cycle (Fig. 6). mutC after four cycles at 90°C retained 35% of the activity while 6B retained only 15% activity. Mass spectrometric analysis was performed on 6B and mutC proteins that were subjected to three heat/cool cycles (Supporting Information Table 2). Multiple deamidations were seen in 6B but not in mutC, indicating accumulation of progressive deamidations in 6B after heat/cool cycles.

Extent of deamidation in mutC after heat treatment

mutC was incubated at elevated temperatures (100°C) followed by trypsin digestion, and mass analysis was performed on ESI nano LC MS/MS as described earlier (Supporting Information Table 3). Deamidation of asparagines at positions 18 and 138 was observed in mutC, after the heat treatment. Apart from initial deamidation at 18, 51, 82, 138, and 174, deamidation at positions 48 and 106 in 6B were more common compared to mutC.

Deamidation of glutamyl and asparaginyl residues in proteins is a physiologically relevant nonenzymatic post-translational modification.[5,9,10,40,41] Deamidation adds a negative charge, which may alter the intramolecular interactions in a protein leading to altered stability, folding, and biological functions of the protein. Deamidation of proteins has a significant role in various biological processes. Deamidation in βA3 crystallins initiates aggregation and precipitation leading to the formation of cataracts.[7,23,42] Deamidation of long-lived self-proteins may qualitatively or quantitatively affect the spectrum of self-displayed peptides to T cells and thus contributing to exacerbation of auto immune diseases.[43,44] It has also been suggested that *in vivo* deamidation of proteins could serve as a molecular timer of many important biological events, such as aging.[5,45–47] Few studies have attempted to investigate the consequences of deamidation by directly investigating the altered properties or by mutating the deamidated site. Deamidation of N7 and N66 led to stabilization of an unfolding intermediate in Barstar.[42] N67 deamidation in ribonuclease A resulted in loss of stability due to loss of two important hydrogen bonds.[48] Triply substituted asparagines (N26D, N26D/N131D) in superoxide dismutase are less stable than the wild-type superoxide dismutase (SOD) and led to rapid formation of amyloid fibrils.[49] Pathogen-mediated deamidation of host proteins was shown to be a subtle and effective way to impart virulence.[13,50]

Discussion

Several factors influence the deamidation kinetics of asparagines including the adjacent amino acid sequences, surrounding amino acids, and pH. An excellent database on the influence of amino acids adjacent to asparagine on its deamidation kinetics was generated using 477 pentapeptides. Based on this database, the deamidation half-life for N51, N82, and N174 were found to be >1, 43.5, and 1.08 days, respectively. Deamidation coefficient is derived by incorporating the 3D structure into the deamidation kinetics.[9] Using the published program, the deamidation coefficients for N51, N82, and N174 were found to be 4.7, 136, and 1.5, respectively (Supporting Information Table 4). Among the three asparagines, only N174 is surface exposed. Deamidation of N82 is poorly predicted. Pentapeptide deamidation kinetics and its derived deamidation coefficient were based on data obtained at room temperature and physiological pH. The deamidation conditions, as followed in this study such as high temperature, could be complex, hence may limit the predictive ability of the software. The decrease in the activity of mutC compared to 6B could be due to N82, which interacts with groups present in the active site, M78 and G79 that are adjacent to the active site S77 (Supporting Information Table 5; Protein Interaction Calculator software).

SSM of deamidated asparagines to improve the thermotolerant properties of proteins has not been reported. Reported studies investigated the properties of deamidated properties or considered N to D substitution as a missense mutation. These studies have reported loss of stability, activity of proteins, and also increased aggregation properties as shown in crystallins,[7,8,11,12,23,24,51–53] superoxide dismutase,[49] and immunoglobins.[14,34,54] Reported properties of mutC suggest that this protein has retained the secondary and tertiary structure with a partial loss in activity but with a significant improvement in the ability to withstand multiple heat cycles.

Materials and Methods

Materials

Taq polymerase and deoxyribonucleotide triphosphates (dNTPs) were purchased from Invitrogen, Carlsbad, CA. Phusion polymerase, restriction enzymes were sourced from New England Bio labs, Ipswich, MA. Rapid T4 DNA ligase was procured from Kapa Bio Systems, MA. PNPA and *p*-nitrophenyl butyrate (PNPB), lysozyme, Triton X-100, bis-ANS were purchased from Sigma, St. Louis, MO. Qiagen miniprep kit, Qia quick gel extraction kit were purchased from Qiagen, limburg, Netherlands.

All other reagents used were of analytical grade or higher and were purchased locally.

Protein purification

Recombinant triple mutant, mutC, was purified by using a modified version of earlier reported protocol.[31] In the modified procedure, only hydrophobic interaction chromatography was done using phenyl sepharose 6 fast flow (high sub) matrix (GE Life Sciences, Piscataway, NJ). Briefly, solvent A and B, composed of 30% and 80% ethylene glycol in 10 m*M* potassium phosphate (pH 7.2), respectively, were used for generating two-step gradient (First step 0–70% of 80% ethylene glycol for 50 mL at 0.3 mL/min flow rate; second step 70–100% of 80% ethylene glycol for 50 mL at a flow rate of 0.2 mL/min). Protein was purified to homogeneity in the first step of the gradient without any requirement for additional purification step as confirmed on a SDS-PAGE gel.

Secondary structure and thermal unfolding/refolding

Far-UV CD of protein was recorded from 250 to 205 nm wavelength in a spectropolarimeter (JASCO J-815) at a protein concentration of 0.05 mg/mL in 50 m*M* sodium phosphate (pH 7.2) in a 1 cm path length cuvette. Data were recorded in continuous mode (scan speed 50 nm/min, response time, 2 sec, band width, 2 nm, and data pitch 0.2 nm). Wavelength scans were averaged from three spectral accumulations. Near-UV CD of protein was recorded from 310 to 250 nm wavelength at a protein concentration of 1 mg/mL in 50 m*M* sodium phosphate buffer at pH 7.2 with same settings as above. Spectra were corrected for buffer baseline by subtracting buffer blank collected under same settings. Mean residue ellipticity was calculated using following equation. $[\theta]_{MRW} = (M_r \times \theta)/(10 \times l \times C)$, where θ is ellipticity in degrees, l is path length in cm, and C is concentration in g/mL. Mean residue weight (M_r) is taken as 115.

Reversibility and thermal melting of 6B and mutC was monitored using spectropolarimeter (JASCO J-815) fitted with Jasco Peltier-type temperature controller (CDF-426S/16). Samples (0.05 mg/mL in 50 m*M* sodium phosphate, pH 7.2) were heated from 25°C to 95°C for unfolding and 95°C to 25°C for refolding at a rate of 1°C/min in a 3 mL cuvette of 1 cm path length. Change in the ellipticity at 222 nm was measured as function of temperature to follow unfolding and refolding transitions. The scans were repeated and confirmed for the absence of aggregation.

Thermal inactivation

50 μL of protein at a concentration of 0.05 mg/mL in 50 m*M* sodium phosphate, pH 7.2 was taken in 0.2 mL microfuge tubes and were incubated in a thermal cycler for precise temperature control. Protein was heated at different temperatures for 20 min, cooled at 4°C for 20 min, and finally equilibrated at 25°C for 15 min. Samples were centrifuged, and activity was determined as described later.

Fluorescence

Bis-ANS binding to protein was measured using a Hitachi F7000 fluorimeter (X-390 nm). Bis-ANS (10 μM) was added to 0.05 mg/— protein in sodium phosphate buffer (50 mM, pH 7.2). Intrinsic fluorescence of lipase was measured by monitoring the tryptophan fluorescence (X-295 nm).

Enzyme activity

Lipase activity was measured by the hydrolysis of the substrate, PNPB (2 mM) in the presence of Triton X-100 (20 mM) and sodium phosphate buffer (50 mM, pH 7.2) at room temperature. The release of *p*-nitrophenol was monitored at 405 nm in a spectrophotometer (Shimadzu UV-Vis Spectrophotometer).

Enzyme kinetics of lipase was measured using PNPA, a soluble substrate of lipase. Using a 200 m*M* stock of PNPA in acetone, a concentration range of 0.2–2 mM was obtained by adding appropriate amount of substrate into 1 mL of 50 m*M* sodium phosphate buffer (pH 7.2) containing 1 μg protein. All activity measurements were made at room temperature. K_{cat}/k_m values were derived from Lineweaver-Burke transformation.

IEF

IEF was performed as described earlier with minor modifications. Thirty microgram of purified protein samples, incubated at elevated temperatures (70–100°C) for 20 min, were mixed with 80 μl of rehydration buffer (8 *M* urea, 50 m*M* dithiothretol (DTT), 2% w/v CHAPS, 0.2% w/v Biolyte (pH 3–10) (BioRad, Richmond, CA) with traces of bromo phenol blue and used to rehydrate immobilized pH gradient (IPG) strips (pH 3–10) overnight. The strips were overlaid with mineral oil to prevent evaporation. After overnight rehydration, the IPG strip was loaded onto an IEF tray (Protean IEF tray, BioRad) with wet paper wicks over the electrode. The focusing conditions were set up according to the manufacturer's instructions. Briefly, one-step ramping protocol was used as the pH range was broad and temperature was maintained at 20°C. The second dimension SDS-PAGE was carried out according to standard procedure.[55] Prior to loading on gel, IPG strips were incubated in equilibration buffers I (6 *M* urea, 2% SDS, 2% DTT, and 20% glycerol in 0.375 *M* Tris-HCl, pH 8) and II (buffer I, containing 2.5% iodoacetamide) for 20 min each, with gentle shaking. The strips were rinsed in 1× Tris-glycine buffer and

loaded on resolving gel followed by sealing with 1% agarose. Rest of the steps was identical to that of SDS-PAGE protocol.

Temperature-induced deamidation and mass spectrometry

Lipase (6B and mutC) were incubated at higher temperatures (80°C, 90°C, and 100°C) for 20 min followed by incubation at 4°C for 20 min and incubation at 25°C for 15 min. 1 μg of protein was subjected to proteolysis using Trypsin Gold by incubating at 37°C for 18 h at an enzyme substrate weight ratio of 1:40.Trypsin digests were then desalted using C18-Ziptip from Millipore (Bedford, MA) using manufacturer recommended protocol. Desalted trypsin digests were subjected to ESI Nano LC-MS/MS analysis in an Orbitrap Velos mass spectrometer (Thermo scientific, Waltham, MA). Briefly, trypsin-digested peptides were suspended in 10 μL of 5% acetonitrile and 0.1% formic acid. Peptides were fractionated on Nano flow LC system (Easy nLCII, Proxeon Bio systems, Odense, Denmark) using Bio Basic C18 Pico Frit Nano capillary column (75 μm × 10 cm: New objective, MA) with a linear gradient of 0–100% B (solvent A: 5% acetonitrile with 0.1% formic acid; solvent B: 95% acetonitrile with 0.1% formic acid) in 60 min, at a flow rate of 200 nL/min, and fractions were analyzed on LTQ Orbitrap Velos (Thermo scientific). 1.7 kV was applied for ionization. Full scan MS with a mass window 300–2000 Da was acquired after accumulation to target value of 1E6 in FT-ICR mode. FT resolution was set to $r = 6E4$, and the top 20 peptides with charge 2 or more were isolated to a target value of 5E3 and fragmented in linear ion trap with normalized collision energy of 35% in CID mode. Fragment ions were scanned in low pressure ion trap at scan rate of 33,333 amu/s, and threshold ion selection for MS/MS was set as 500 counts. Ion accumulation times were set at 500 ms for MS and 25 ms for MS/MS. Activation time of 10 ms and activation q value (collision endothermicity) of 0.25 was used.

Analysis of mass data

SEQUEST search. SEQUEST HT search was performed using proteome Discoverer 1.4 ver. 1.4.0.288 platform of Thermo Scientific. Raw file was analyzed against NCBI nr Database *Bacillus subtilis* species. For both 6B and mutC, methionine oxidation and deamidation of asparagine and glutamine were set as variable modifications. Trypsin was set as protease allowing up to three missed cleavages, peptide length was set at ≥4, parent ion tolerance was set at 10 ppm, and fragment ion tolerance was set at 0.6 ppm. FDR-based statistics were calculated for the raw spectra for high confidence protein assignment to a P value of 0.01.

Peaks DB search. Raw files were also analyzed using a database search engine from PEAKS (ver. 6.0). Advantage of PEAKS lies in its ability to preprocess spectra to give a high quality mass spectra of identified proteins and also integrate de novo results to validate peptide spectrum matches in protein identification. Data preprocessing was done using following settings: precursor ion and fragment ion tolerance was set at 10 ppm and 0.6 Da, respectively. Peptides with +1 to +4 charges, precursor mass in the range of 250–5000 Da, and retention time window of 0.5–59.5 min were considered for protein identification. Spectral quality was set at 0.65 as recommended by the manufacturer. Database search was done against *Bacillus subtilis* species from NCBI database. $-10\log P$ scores were set in such a way that the FDR value reaches a theoretical value of zero.

Plasmid isolation and sequencing

Plasmid DNA from BL21 (DE3) *E. coli* was isolated using QIA prep Miniprep kit. Sequencing was done by using T7 promoter (T7PP) and T7 terminator (T7TP) primers. Sequencing reaction consisted of 25 ng of template DNA, 2.5 picomoles of each primer, sequencing buffer, and Big Dye reagent (Applied Biosystems, Foster City, CA). Reactions were carried out for 30 cycles of 94°C for 10 sec, 52°C for 5 sec followed by 60°C for 4 min in a polymerase chain reaction (PCR) thermal cycler. Sequencing was done using ABI 3730 sequence analyzer (Applied Biosystems).

Recombination of mutations

Triple mutant was generated in the background of N51E lipase template, two mutations N82H, N174S were incorporated. Briefly, first PCR was done using a combination of N82HR/T7PP, N82HF/N174SR, N174S/T7TP forward and reverse primers, the amplicons obtained were purified with QIA gel extraction kit. Overlay extension PCR was done using the purified fragments to generate full-length lipase gene.

For overexpression and purification of the mutant lipase, the gene was amplified using pET22NDEF as forward and T7TP as reverse primers, and the PCR product thus obtained was gel extracted and subjected to restriction digestion using restriction enzymes NdeI and HindIII. Double digested product was purified and ligated to similarly digested pET21b vector using Kapa T4 DNA ligase. Ligated product was purified after gel extraction and transformed into *E. coli* BL21 (DE3) competent cells.

SSM

SSM was performed using a pair of oligonucleotide primers. The amino acid position targeted were

coded by NNK (sense strand) and MNN (antisense strand), where N = A, G, C, or T, K = G or T and M = A or C. The overlap extension was carried out with vector-specific primers, that is, T7 promoter and T7 terminator, in combination with position-specific mutagenic primers using pET22b-6B as template.

Mutagenic PCR product and pET22b vector was double digested with NcoI, HindIII and ligated using Kapa T4 DNA ligase. Mutagenic product thus obtained was transformed into *E. coli* BL21 (DE3) competent cells. Cells were plated on petriplate containing Luria Bertani (LB) (1% tryptone, 0.5% yeast extract, and 1% NaCl) agar with 100 μg/mL ampicillin.

Screening of SSM population

Improvement in the residual activity of the mutants was analyzed by following a two tier screening methodology. Initial coarse screen was done on 96-well plates followed by a stringent second screen of clones derived from coarse screen. About 200 colonies per each position from the petriplate containing transformants were randomly selected. Cells were inoculated into individual wells in a 96-well plates containing LB medium with 100 μg/mL ampicillin. Plates were incubated in a shaker incubator at 37°C at 200 rpm for 6 h. This culture was then used to inoculate fresh medium in identical plates. Following inoculation, cultures were grown for 6 h at 37°C, 200 rpm. IPTG was added to each well after 6 h to a final concentration of 0.5 m*M* and incubated for 12 h. Cells were pelleted by spinning the culture at 4000 rpm for 30 min at 4°C, the supernatant was mixed (1:8) with 100 m*M* sodium phosphate buffer (pH 7.2), and split into wells into three identical 96-well PCR plates (Axygen Scientific, Union city, CA). One plate was incubated at 95°C for 30 min, cooled at 4°C for 20 min followed by equilibration at 25°C for 15 min in a PCR thermal cycler (GeneAmp 9700, Applied Biosystems), and the second plate was incubated at 85°C, with cooling and equilibration time similar to first one. Third plate was subjected to only cooling and equilibration steps similar to plate one and two.

Activity measurements were performed by mixing 80 μL of diluted culture supernatant with 80 μL of 2× PNPB-Triton X-100 substrate (4 m*M* PNPB micellized in 40 m*M* Triton X-100 in sodium phosphate buffer [pH 7.2]). Increment in the absorbance at 405 nm with time was monitored using Spectramax 190 plate reader (Molecular Devices, Sunnyvale, CA). Data were analyzed using SoftMaxPro 4.7.1 software provided with the instrument. Positive clones are selected based on the ratio of residual activity at higher temperature versus activity at room temperature. Positive clones selected in the first round were confirmed by subjecting to a second tier screening, where in each clone was assayed in six wells.

Thermal tolerance of lipase

Activity assay. Proteins at a concentration of 0.05 mg/mL in 50 m*M* sodium phosphate, at pH 7.2 were incubated at 90°C for 30 min, cooled to 4°C for 20 min, and equilibrated at 25°C for 15 min. Following incubation, sample was centrifuged and activity in the supernatant was determined. Either for 6B or mutC, any loss of protein due to aggregation after the heat/cool cycles was not observed. Same cycle was repeated, and the residual activity after each cycle was measured. Proteins (6B and mutC) from the fourth cycle were subjected to in-solution digestion by overnight (~18 h) incubation with Trypsin Gold (Promega, Madison, WI) in 50 m*M* acetic acid at 37°C followed by mass spectrometric analysis as described earlier.

Conclusion

Replacement of asparagines that are susceptible to temperature-induced deamidation with amino acids identified by SSM resulted in a thermotolerant lipase. The resultant triple mutant has retained the native structure and enhanced tolerance to heat/cool cycles. This study highlights importance of *in vitro* evolution approaches to recover deamidation-mediated loss in protein structure/function and argues for efficient predictive software for protein deamidation under different stress conditions in proteins, that is, temperature, pH, solvent, and so on.

Acknowledgment

The authors acknowledge the help of Mr. CVB Swamy for his support in mass spectrometry work.

References

1. Pace CN, Hermans J (1975) The stability of globular protein. Crit Rev Biochem Mol Biol 3:1–43.
2. Tomazic SJ, Klibanov AM (1988) Why is one Bacillus alpha-amylase more resistant against irreversible thermoinactivation than another? J Biol Chem 263:3092–3096.
3. Zhou XX, Wang YB, Pan YJ, Li WF (2008) Differences in amino acids composition and coupling patterns between mesophilic and thermophilic proteins. Amino Acids 34:25–33.
4. Metpally RP, Reddy BV (2009) Comparative proteome analysis of psychrophilic versus mesophilic bacterial species: insights into the molecular basis of cold adaptation of proteins. BMC Genom 10:11.
5. Hains PG, Truscott RJ (2010) Age-dependent deamidation of lifelong proteins in the human lens. Invest Ophthalmol Vis Sci 51:3107–3114.
6. Pace AL, Wong RL, Zhang YT, Kao YH, Wang YJ (2013) Asparagine deamidation dependence on buffer type, pH, and temperature. J Pharm Sci 102:1712–1723.

7. Takata T, Oxford JT, Brandon TR, Lampi KJ (2007) Deamidation alters the structure and decreases the stability of human lens betaA3-crystallin. Biochemistry 46:8861–8871.
8. Flaugh SL, Mills IA, King J (2006) Glutamine deamidation destabilizes human gammaD-crystallin and lowers the kinetic barrier to unfolding. J Biol Chem 281: 30782–30793.
9. Robinson NE, Robinson AB (2001) Deamidation of human proteins. Proc Natl Acad Sci USA 98:12409–12413.
10. Weintraub SJ, Manson SR (2004) Asparagine deamidation: a regulatory hourglass. Mech Ageing Dev 125: 255–257.
11. Takemoto L, Boyle D (2000) Increased deamidation of asparagine during human senile cataractogenesis. Mol Vis 6:164–168.
12. Zhang Z, Smith DL, Smith JB (2003) Human beta-crystallins modified by backbone cleavage, deamidation and oxidation are prone to associate. Exp Eye Res 77: 259–272.
13. Washington EJ, Banfield MJ, Dangl JL (2013) What a difference a Dalton makes: bacterial virulence factors modulate eukaryotic host cell signaling systems via deamidation. Microbiol Mol Biol Rev 77:527–539.
14. Dan A, Takahashi M, Masuda-Suzukake M, Kametani F, Nonaka T, Kondo H, Akiyama H, Arai T, Mann DM, Saito Y, Hatsuta H, Murayama S, Hasegawa M (2013) Extensive deamidation at asparagine residue 279 accounts for weak immunoreactivity of tau with RD4 antibody in Alzheimer's disease brain. Acta Neuropathol Commun 1:54.
15. Capasso S, Mazzarella L, Sica F, Zagari A (1989) Deamidation via cyclic imide in asparaginyl peptides. Pept Res 2:195–200.
16. Catak S, Monard G, Aviyente V, Ruiz-Lopez MF (2009) Deamidation of asparagine residues: direct hydrolysis versus succinimide-mediated deamidation mechanisms. J Phys Chem A 113:1111–1120.
17. Capasso S, Di CP (2000) Kinetic and thermodynamic control of the relative yield of the deamidation of asparagine and isomerization of aspartic acid residues. J Pept Res 56:382–387.
18. Li B, Gorman EM, Moore KD, Williams T, Schowen RL, Topp EM, Borchardt RT (2005) Effects of acidic N + 1 residues on asparagine deamidation rates in solution and in the solid state. J Pharm Sci 94:666–675.
19. Robinson AB, Rudd CJ (1974) Deamidation of glutaminyl and asparaginyl residues in peptides and proteins. Curr Top Cell Regul 8:247–295.
20. Robinson NE, Robinson AB (2001) Prediction of protein deamidation rates from primary and three-dimensional structure. Proc Natl Acad Sci USA 98:4367–4372.
21. Robinson NE, Robinson AB (2004) Prediction of primary structure deamidation rates of asparaginyl and glutaminyl peptides through steric and catalytic effects. J Pept Res 63:437–448.
22. Tyler-Cross R, Schirch V (1991) Effects of amino acid sequence, buffers, and ionic strength on the rate and mechanism of deamidation of asparagine residues in small peptides. J Biol Chem 266:22549–22556.
23. Takata T, Oxford JT, Demeler B, Lampi KJ (2008) Deamidation destabilizes and triggers aggregation of a lens protein, betaA3-crystallin. Protein Sci 17:1565–1575.
24. Gupta R, Srivastava OP (2004) Effect of deamidation of asparagine 146 on functional and structural properties of human lens alphaB-crystallin. Invest Ophthalmol Vis Sci 45:206–214.
25. Chen HM, Ford C, Reilly PJ (1994) Substitution of asparagine residues in *Aspergillus awamori* glucoamylase by site-directed mutagenesis to eliminate N-glycosylation and inactivation by deamidation. Biochem J 301:275–281.
26. Friedman AR, Ichhpurani AK, Brown DM, Hillman RM, Krabill LF, Martin RA, Zurcher-Neely HA, Guido DM (1991) Degradation of growth hormone releasing factor analogs in neutral aqueous solution is related to deamidation of asparagine residues. Replacement of asparagine residues by serine stabilizes. Int J Pept Protein Res 37:14–20.
27. Ahmad S, Kumar V, Ramanand KB, Rao NM (2012) Probing protein stability and proteolytic resistance by loop scanning: a comprehensive mutational analysis. Protein Sci 21:433–446.
28. Kumar V, Yedavalli P, Gupta V, Rao NM (2014) Engineering lipase A from mesophilic *Bacillus subtilis* for activity at low temperatures. Protein Eng Des Sel 27: 73–82.
29. Molloy EM, Field D, O' Connor PM, Cotter PD, Hill C, Ross RP (2013) Saturation mutagenesis of lysine 12 leads to the identification of derivatives of nisin A with enhanced antimicrobial activity. PLoS One 8:e58530.
30. Tripathi A, Varadarajan R (2014) Residue specific contributions to stability and activity inferred from saturation mutagenesis and deep sequencing. Curr Opin Struct Biol 24:63–71.
31. Kamal MZ, Ahmad S, Molugu TR, Vijayalakshmi A, Deshmukh MV, Sankaranarayanan R, Rao NM (2011) In vitro evolved non-aggregating and thermostable lipase: structural and thermodynamic investigation. J Mol Biol 413:726–741.
32. Ahmad S, Kamal MZ, Sankaranarayanan R, Rao NM (2008) Thermostable *Bacillus subtilis* lipases: in vitro evolution and structural insight. J Mol Biol 381:324–340.
33. Krokhin OV, Antonovici M, Ens W, Wilkins JA, Standing KG (2006) Deamidation of -Asn-Gly- sequences during sample preparation for proteomics: consequences for MALDI and HPLC-MALDI analysis. Anal Chem 78:6645–6650.
34. Diepold K, Bomans K, Wiedmann M, Zimmermann B, Petzold A, Schlothauer T, Mueller R, Moritz B, Stracke JO, Molhoj M, Reusch D, Bulau P (2012) Simultaneous assessment of Asp isomerization and Asn deamidation in recombinant antibodies by LC-MS following incubation at elevated temperatures. PLoS One 7:e30295.
35. Hao P, Ren Y, Alpert AJ, Sze SK (2011) Detection, evaluation and minimization of nonenzymatic deamidation in proteomic sample preparation. Mol Cell Proteomics 10:O111.
36. Kameoka D, Ueda T, Imoto T (2003) A method for the detection of asparagine deamidation and aspartate isomerization of proteins by MALDI/TOF-mass spectrometry using endoproteinase Asp-N. J Biochem 134: 129–135.
37. Cournoyer JJ, Pittman JL, Ivleva VB, Fallows E, Waskell L, Costello CE, O'Connor PB (2005) Deamidation: differentiation of aspartyl from isoaspartyl products in peptides by electron capture dissociation. Protein Sci 14:452–463.
38. Ni W, Dai S, Karger BL, Zhou ZS (2010) Analysis of isoaspartic Acid by selective proteolysis with Asp-N and electron transfer dissociation mass spectrometry. Anal Chem 82:7485–7491.
39. Chin IS, Murad AMA, Mahadi NM, Nathan S, Bakar FDA (2013) Thermal stability engineering of Glomerella cingulata cutinase. Prot Engin Des Sel 26:369–375.

40. Catterall JB, Hsueh MF, Stabler TV, McCudden CR, Bolognesi M, Zura R, Jordan JM, Renner JB, Feng S, Kraus VB (2012) Protein modification by deamidation indicates variations in joint extracellular matrix turnover. J Biol Chem 287:4640–4651.
41. Reissner KJ, Aswad DW (2003) Deamidation and isoaspartate formation in proteins: unwanted alterations or surreptitious signals? Cell Mol Life Sci 60:1281–1295.
42. Jha SK, Deepalakshmi PD, Udgaonkar JB (2012) Characterization of deamidation of barstar using electrospray ionization quadrupole time-of-flight mass spectrometry, which stabilizes an equilibrium unfolding intermediate. Protein Sci 21:633–646.
43. Sollid LM, Jabri B (2013) Triggers and drivers of autoimmunity: lessons from coeliac disease. Nature Rev Immun 13:294–302.
44. Moss CX, Matthews SP, Lamont DJ, Watts C (2005) Asparagine deamidation perturbs antigen presentation on class II major histocompatibility complex molecules. J Biol Chem 280:18498–18503.
45. Hooi MY, Raftery MJ, Truscott RJ (2012) Racemization of two proteins over our lifespan: deamidation of asparagine 76 in gammaS crystallin is greater in cataract than in normal lenses across the age range. Invest Ophthalmol Vis Sci 53:3554–3561.
46. Robinson AB, McKerrow JH, Cary P (1970) Controlled deamidation of peptides and proteins: an experimental hazard and a possible biological timer. Proc Natl Acad Sci USA 66:753–757.
47. van Doorn NL, Wilson J, Hollund H, Soressi M, Collins MJ (2012) Site-specific deamidation of glutamine: a new marker of bone collagen deterioration. Rapid Commun Mass Spectrom 26:2319–2327.
48. Capasso S, Di DA, Esposito L, Sica F, Sorrentino G, Vitagliano L, Zagari A, Mazzarella L (1996) Deamidation in proteins: the crystal structure of bovine pancreatic ribonuclease with an isoaspartyl residue at position 67. J Mol Biol 257:492–496.
49. Shi Y, Rhodes NR, Abdolvahabi A, Kohn T, Cook NP, Marti AA, Shaw BF (2013) Deamidation of asparagine to aspartate destabilizes Cu, Zn superoxide dismutase, accelerates fibrillization, and mirrors ALS-linked mutations. J Am Chem Soc 135:15897–15908.
50. Doye A, Mettouchi A, Bossis G, Clément R, Buisson-Touati C, Flatau G, Gagnoux L, Piechaczyk M, Boquet P, Lemichez E (2002) CNF1 exploits the ubiquitin-proteasome machinery to restrict Rho GTPase activation for bacterial host cell invasion. Cell 111:553–564.
51. Gupta R, Srivastava OP (2004) Deamidation affects structural and functional properties of human alphaA-crystallin and its oligomerization with alphaB-crystallin. J Biol Chem 279:44258–44269.
52. Hanson SR, Hasan A, Smith DL, Smith JB (2000) The major in vivo modifications of the human water-insoluble lens crystallins are disulfide bonds, deamidation, methionine oxidation and backbone cleavage. Exp Eye Res 71:195–207.
53. Takemoto L (1999) Increased deamidation of asparagine-101 from alpha-A crystallin in the high molecular weight aggregate of the normal human lens. Exp Eye Res 68:641–645.
54. Powell BS, Enama JT, Ribot WJ, Webster W, Little S, Hoover T, Adamovicz JJ, Andrews GP (2007) Multiple asparagine deamidation of *Bacillus anthracis* protective antigen causes charge isoforms whose complexity correlates with reduced biological activity. Proteins 68: 458–479.
55. Sambrook J, Fritsch EF, Maniatis T (1989) Molecular cloning. Cold Spring Harbor Laboratory Press, New York.